Article

pubs.acs.org/Biomac

Cooperative Self-Assembly of Peptide Gelators and Proteins

Nadeem Javid,[†] Sangita Roy,[†] Mischa Zelzer,[†] Zhimou Yang,[‡] Jan Sefcik,*[,§] and Rein V. Ulijn*[,†]

[†]WestCHEM, Department of Pure and Applied Chemistry, University of Strathclyde, Glasgow, U.K.

[‡]State Key Laboratory of Medicinal Chemical Biology, College of Life Sciences, Nankai University, Tianjin 300071, China

[§]Department of Chemical and Process Engineering, University of Strathclyde, Glasgow, U.K.

Supporting Information

ABSTRACT: Molecular self-assembly provides a versatile route for the production of nanoscale materials for medical and technological applications. Herein, we demonstrate that the cooperative self-assembly of amphiphilic small molecules and proteins can have drastic effects on supramolecular nanostructuring of resulting materials. We report that mesoscale, fractal-like clusters of proteins form at concentrations that are orders of magnitude lower compared to those usually associated with molecular crowding at room temperature. These protein clusters have pronounced effects on the molecular self-assembly of aromatic peptide amphiphiles (fluorenylmethoxycarbonyl- dipeptides), resulting in a reversal of chiral organization and enhanced order through templating and binding. Moreover, the morphological and mechanical properties of the resultant nanostructured gels can be controlled by the cooperative self-assembly of peptides and protein fractal clusters, having implications for biomedical applications where proteins and peptides are both present. In addition, fundamental insights into cooperative interplay of molecular interactions and confinement by clusters of chiral macromolecules is relevant to gaining understanding of the molecular mechanisms of relevance to the origin of life and development of synthetic mimics of living systems.

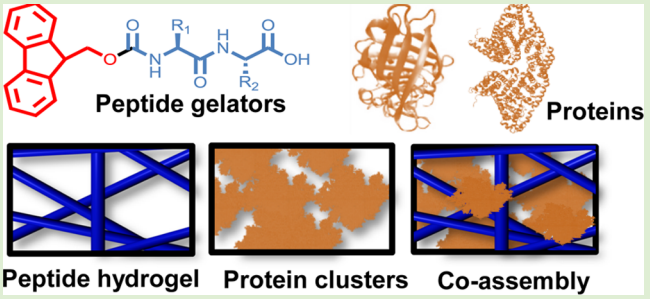

INTRODUCTION

Molecular self-assembly provides a versatile route for the production of nanoscale materials for biomedical and technological applications.[1−3] In the laboratory, molecular self-assembly is often carried out in dilute solutions while in biological contexts it takes place in the highly complex and crowded environment of the cytoplasm or tissue fluids.[4] It is understood that this environment can have a substantial effect on molecular self-assembly processes, e.g., through excluded volume effects, binding and templating.[5,6] The effects of macromolecular confinements on supramolecular self-assembly and small molecule gelation have been rarely studied. Formation of disordered aggregates, mesoscale networks, and self-assembled structures, including amyloid spherulites and protein fibers have been reported at high concentrations, at elevated temperatures or at reduced pH.[7−13]

Mixing of macromolecules and small molecules can dramatically alter molecular assembly through cooperative behavior. For example, Stupp et al. have shown that interfacial macroscopic membranes can be generated by mixing high molecular weight polysaccharide hyaluronic acid with peptide amhiphiles.[14] It has been demonstrated that the addition of a polysaccharides (dextran)[15a] or clay particles[15b] can alter the mechanical properties of small molecule hydrogels. On the other hand, it has been demonstrated that certain gelators and surfactants can self-assemble orthogonally.[16a] Recently, Xu et al. have shown that amphiphilic peptides interact and bind with cytosol proteins in a drastically different manner depending upon their nanoscale structure.[16b]

We set out to examine the ability of dilute protein clusters (at concentrations that are much lower compared to those usually associated with molecular crowding) to modulate the self-assembly of peptide based gelators through templating and binding effects. A small set of amphiphilic peptide gelators were selected based on the differences in hydrophobicity and hydrogen bonding capabilities (the main driving forces in the self-assembly of aromatic peptide amphiphiles)[3e] and two structurally different proteins (with different hydropathy indices) were selected to study cooperativity in peptide/protein coassembly. We demonstrate that small molecule self-assembly (in this case a range of aromatic peptide amphiphiles, fluorenylmethoxycarbonyl-dipeptides with varying polarity, Scheme 1) can be dramatically influenced and directed by the presence of up to 0.2 wt % protein clusters (bovine serum albumin and β-lactoglobulin). Scattering and spectroscopy methods are used to assess the influence of protein templating on supramolecular ordering. In addition to new fundamental insights into cooperative interplay of molecular interactions and confinement by clusters of chiral macromolecules that arise from this work, the approach provides simple methodology to

Received: September 3, 2013
Revised: November 6, 2013
Published: November 20, 2013

Scheme 1. (a) Low Molecular Weight Hydrogelators (Fmoc-Dipeptides), (b) Protein Structures of β-LG/BSA Used in the Study and Their Hydropathy Indices (hI) and Isoelectric Points (pI), (c) Supramolecular Assembly of Peptides Resulting in Fibrous Structures and Proteins Yielding Mesoscale Fractal Clusters[a]

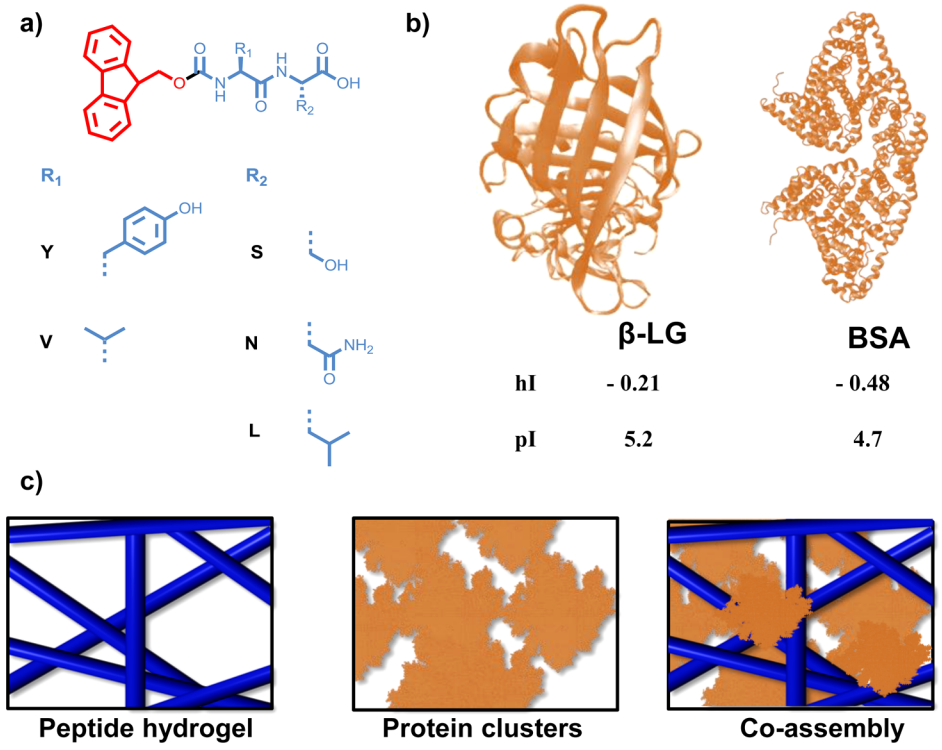

[a]The hydropathy index (hI) was calculated using "grand average hydropathy (GRAVY)".[17]

enable production of soft materials with tunable structural, mechanical, and chiroptical properties. To our knowledge, this is the first report to utilize dilute disordered protein clusters as a tool for multifaceted modulation of the self-assembly process.

EXPERIMENTAL SECTION

1.1. Formation of Supramolecular Hydrogel. The self-assembling systems used in this study are based on aromatic peptide amphiphiles, namely, Fmoc-YL, Fmoc-YN, Fmoc-YS, and Fmoc-VL (Scheme 1) (the detailed synthesis procedure and characterization is described elsewhere).[3e] The molecular self-assembly (and gelation) of peptides is induced by sonicating and vortexing the Fmoc-dipeptides (10 mM) in 100 mM sodium phosphate buffer (pH 8) solution with (or without) the addition of various concentrations of proteins β-lactoglobulin (β-LG) and Bovine serum albumin (BSA) in the range of 0.03 to 0.2 wt %. The gelation was initially confirmed by vial inversion and later by oscillatory rheology. In the absence of protein, the Fmoc-dipeptides formed gel within 2 h after sonication and vortexing. Reduced gelation kinetics were observed in the presence of protein, with the Fmoc-dipeptide solutions with added proteins forming gels in 3−6 h depending upon the protein concentration. This reduction in gelation kinetics is possibly due to the difference in nucleation and elongation of fibril formation in the presence of protein, which later entangle to form network of fibers resulting in hydrogelation.

The gels were prepared in UV-grade cuvettes for fluorescence, rheology and AFM measurements. For circular dichroism (CD) spectroscopy Fmoc-dipeptide solutions with and without proteins were dissolved in buffer solutions in glass vials and then quickly transferred to CD cell. All measurements were conducted after 24−27 h of gelation time.

1.2. Fluorescence Emission Spectroscopy. Fluorescence emission spectra were measured on a Jasco FP-6500 spectrofluorometer with light measured orthogonally to the excitation light, at a scanning speed of 100 nm min^{-1}. The excitation wavelength was 280 nm and emission data were recorded in the range between 300 and 600 nm for Fmoc-dipeptide systems with or without added different concentrations of protein. The spectra were measured with a bandwidth of 3 nm with a medium response and a 1 nm data pitch.

1.3. Circular Dichroism (CD). Spectra were measured on a Jasco J600 spectropolarimeter with 1 s integrations with a step size of 1 nm and a single acquisition with a slit width of 1 nm. A circular CD cell (Hellma) was used with a path length of 0.1 mm. The CD cuvette was rotated to measure CD spectra at different angles to ensure no LD artifacts were present in the spectra. All the measured CD spectra had values of HT lower than saturation at all wavelengths in all the gels.

1.4. Rheology. Rheological properties were assessed using an Malvern Kinexus rheometer with temperature controlled at 25 °C using a 20 mm parallel plate geometry with a gap of 0.5 mm. Viscometry measurements were taken by monitoring the viscosity and shear stress over controlled shear rates from 0.1−100 s^{-1}. The dynamic moduli of the hydrogel were measured as a function of frequency in the range of 0.1−100 rad s^{-1} with constant strain value. To ensure the measurements were made in the linear viscoelastic regime, amplitude sweeps were performed at constant frequency of 1 Hz, from shear strain 0.01−100%, where no variation in G' or G'' was observed.

1.5. Atomic Force Microscopy (AFM). For AFM experiments, 50 μL of sample (gel) was dissolved in 950 μL of deionized water and then deposited onto a freshly cleaved mica surface (G250−2 Mica sheets 1″ × 1″ × 0.006″; Agar Scientific Ltd., Essex, U.K.). Each sample was air-dried for 24 h before AFM imaging. The images were obtained by scanning the mica surface in air under ambient conditions using a Veeco diINNOVA scanning probe microscope (VEECO/BRUKER, Santa Barbara, CA) operated in tapping mode. The AFM measurements were obtained using sharp silicon probes (RTESPA; Veeco Instruments SAS, Dourdan, France). AFM scans were taken at 512 × 512 pixels resolution and produced topographic images of the samples in which the brightness of features increases as a function of height.

dx.doi.org/10.1021/bm401319c | Biomacromolecules 2013, 14, 4368−4376

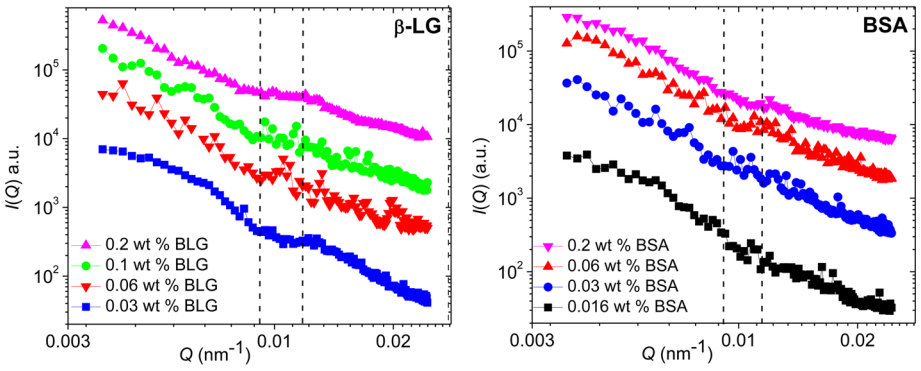

Figure 1. Static light scattering intensity patterns for different concentrations of β-LG and BSA in 100 mM phosphate buffer at pH 8 and room temperature.

Table 1. Apparent Fractal Dimensions (d_f) of Mesoscale Clusters for Various Concentrations of BSA and β-LG Calculated from Static Light Scattering Intensity Patterns at Room Temperature in 100 mM Phosphate Buffer at pH 8

	BSA				β-LG			
concentration (wt %)	0.016	0.03	0.06	0.2	0.03	0.06	0.1	0.2
d_f (Q below 0.01 nm^{-1})	–	2.8 ± 0.1	2.8 ± 0.1	2.7 ± 0.2	–	2.5 ± 0.1	2.8 ± 0.2	2.8 ± 0.3
d_f (Q above 0.01 nm^{-1})	2.1 ± 0.2	2.4 ± 0.1	2.3 ± 0.1	1.5 ± 0.2	3.3 ± 0.3	1.9 ± 0.1	1.9 ± 0.2	1.9 ± 0.2

1.6. Scattering Measurements. The dynamic and static light scattering (DLS and SLS) measurements were carried out by using a 3 DDLS spectrophotometer (LS instruments, Fribourg, Switzerland) using vertically polarized He−Ne laser light (25 mW with wavelength of 632.8 nm) with an avalanche photodiode detector at angles between 15° and 135° at 25 °C. The background scattering intensities (of the buffer) were subtracted from the scattering intensities of the protein solutions. Intensity autocorrelation functions were recorded in dynamic light scattering experiments and analyzed by means of the cumulant method in order to determine the intensity weighted diffusion coefficients D and the average hydrodynamic radius R_h by using the Stokes−Einstein equation, $R_h = k_BT/6\pi\eta D$, where k_B is the Boltzmann constant, T is the absolute temperature and η is the solvent viscosity at the given temperature.

The scattering intensity patterns from static light scattering experiments can be described as $I(Q) \sim KP(Q)S(Q)$, where K is a constant or scaling factor dependent on instrument (and sample species), $P(Q)$ is form factor which depends on the size and shape of the primary particles and $S(Q)$ is structure factor giving information about the spatial arrangement of the primary particles at larger length scales than that of the individual particles.

In the limit of $QR_g \leq 1.2$ the mean radius of gyration (R_g) of individual particles or clusters can be determined by using Guinier's analysis. In the limit $QR \gg 1$ the structure factor dependence upon Q for fractal-like clusters (where R is the radius of primary particles forming the cluster) can be expressed through a power law relationship as $S(Q) \sim Q^{-d_f}$, where d_f is the apparent fractal dimension of the cluster. The fractal cluster structure (shown in Scheme 1) was modeled via diffusion limited aggregation of spheres on a three-dimensional grid using a C++-based algorithm with a sticking coefficient of 0.1 and a unit distance (u.d.) of 1 between the grid points.

RESULTS AND DISCUSSION

Two common proteins, bovine β-lactoglobulin (β-LG) and bovine serum albumin (BSA) were used under near physiological conditions at concentrations up to 0.2 weight% at room temperature. These were coassembled with a series of 9-fluorenylmethoxycarbonyl- (Fmoc-) dipeptides covering a range of chemical properties (Scheme 1; we studied Fmoc-YN, -YS, -YL and -VL with partition coefficients (cLogP) calculated using ChemBiodraw Ultra 12.0 as 2.7, 2.9, 5.5, and 5.6).

Protein Clustering. Protein clustering in buffer solution was first studied in the absence of Fmoc-dipeptides. We used static light scattering (SLS) and dynamic light scattering (DLS) to demonstrate formation of mesoscale protein clusters. Two globular proteins used here are structurally different; bovine β-LG is β-sheet rich and bovine serum albumin (BSA) is α-helix rich (Scheme 1b). Both proteins are anionic at physiological pH and have substantially different hydropathy indices which are of value −0.21 for β-LG and −0.48 for BSA, indicating that β-LG is more hydrophobic in nature. At 0.2 wt % protein concentrations in 10 mM phosphate buffer, native β-LG and BSA exist with hydrodynamic radii 3 and 2.7 nm, respectively as confirmed by DLS (shown in Figure S1, Supporting Information). At higher phosphate buffer concentration of 100 mM, β-LG self-associated to form mesoscale disordered clusters at length-scales of hundreds of nanometers, as evidenced by light scattering intensity patterns showing power-law dependence on Q, the scattering vector magnitude, for Q below 0.01 nm^{-1} (Figure 1).

The internal structure of these clusters is formed by low-density, fractal-like clusters as indicated by power-law scaling exponents of around 2 for Q above 0.01 nm^{-1}, reported as apparent mass fractal dimensions in Table 1. At the lowest protein concentration used, 0.03 wt %, β-LG clusters appear to be smaller, more compact and/or less interconnected as indicated by a gradually flattening pattern of scattered intensity at smaller Q values (The scattering pattern is similar to the structure factor of spherical particle at 0.03 wt % concentration of protein and due to this reason we did not apply the fractal analysis in low Q region and due to the same reason high d_f is obtained in high Q region). Similarly, BSA molecules formed disordered mesoscale clusters at length scales of hundreds of nanometers, showing power-law scaling for Q below 0.01 nm^{-1} (Figure 1) for higher protein concentrations, while again smaller clusters and/or less interconnected arrangement is seen at the lowest protein concentration. The internal structure of BSA clusters shows a dependence on protein concentration in terms of the power-law scaling exponent for Q above 0.01 nm^{-1}, indicating that clusters become more compact at lower

dx.doi.org/10.1021/bm401319c | Biomacromolecules 2013, 14, 4368−4376

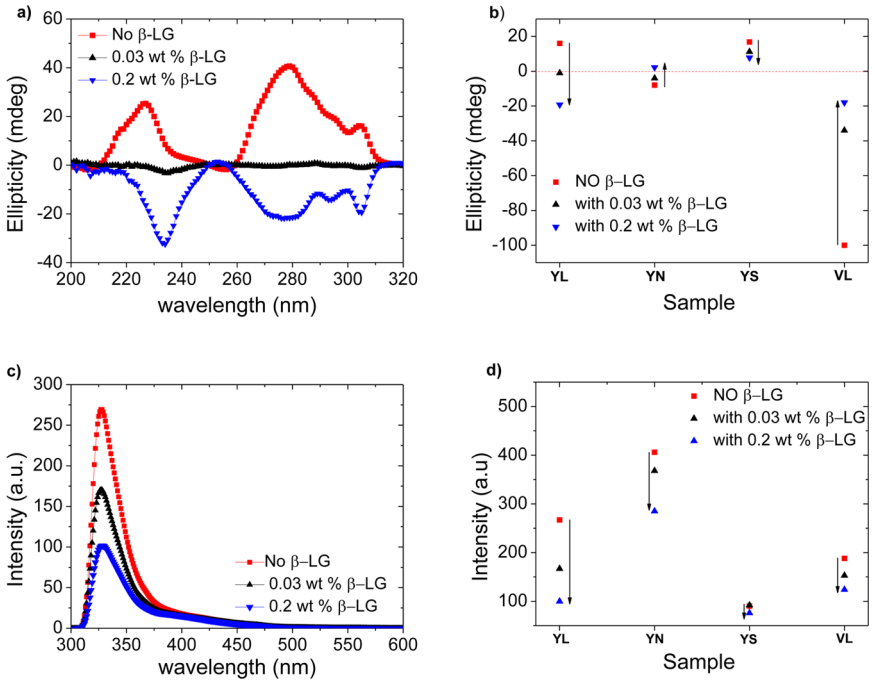

Figure 2. Spectroscopic characterization of Fmoc-dipeptides self-assembly with/without the addition of various concentrations of *β*-LG: (a) CD spectra of Fmoc-YL self-assembly. (b) Effect of protein clusters on ellipticity (at wavelength of 302 nm due to Fmoc-group) for different Fmoc-dipeptides. (c) Fluorescence spectra of Fmoc-YL self-assembly. (d) Effect of protein clusters on fluorescence intensity for different Fmoc-dipeptides.

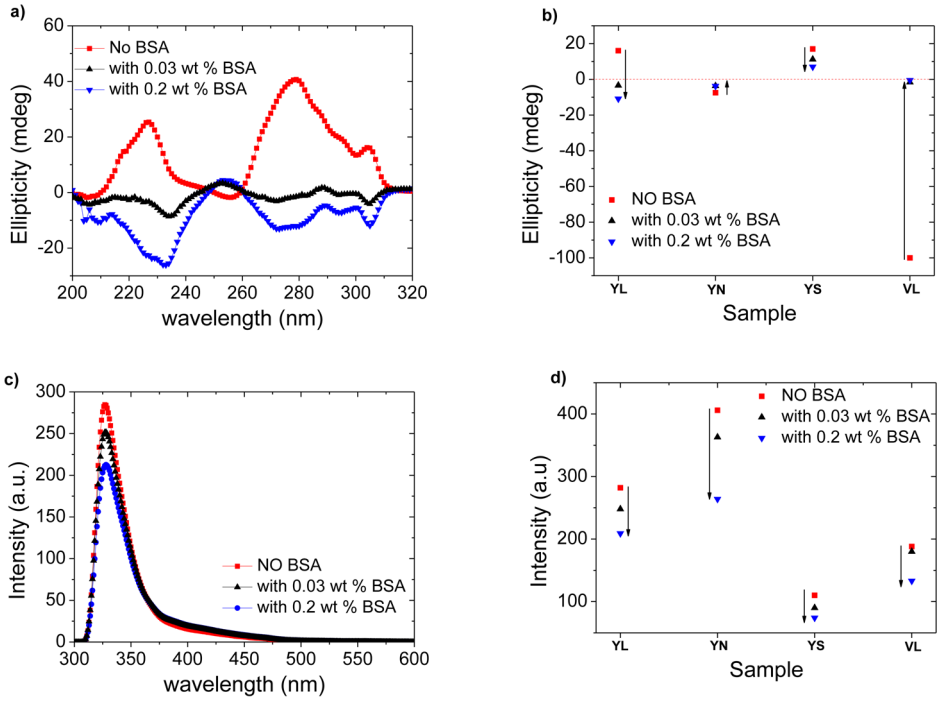

Figure 3. Spectroscopic characterization of Fmoc-dipeptides self-assembly with/without the addition of various concentrations of BSA: (a) CD spectra of Fmoc-YL self-assembly. (b) Effect of protein clusters on ellipticity (at wavelength of 302 nm due to Fmoc-group) for different Fmoc-dipeptides. (c) Fluorescence spectra of Fmoc-YL self-assembly. (d) Effect of protein clusters on fluorescence intensity for different Fmoc-dipeptides.

BSA concentrations. These results demonstrate that supramolecular protein clusters can be formed at much lower protein concentrations under near physiological conditions and at ambient temperature compared to previously reported conditions to obtain protein clusters, e.g. high protein concentrations (4−40 wt %), acidic pH conditions (pH 2.0) and high temperature (40−70 °C) as reported previously.[7−10]

Crucially, the presence of these fractal-like clusters results in slower relaxation of density fluctuations due to restricted mobility of protein molecules within clusters as revealed by DLS autocorrelation function measurements showing power law decay behavior (shown in Figure S2).[18] Unlike protein aggregates under denaturation conditions, the protein clusters observed here are self-associated disordered structures

dx.doi.org/10.1021/bm401319c | *Biomacromolecules* 2013, 14, 4368−4376

composed of native proteins. The slower relaxation dynamics of these protein clusters could reasonably be expected to influence (by restricting mobility and compartmentalization) the coassembly of peptide fibres and protein clusters.

Cooperative Assembly of Fmoc-Peptides and Proteins: Chirality. The cooperative self-assembly of various Fmoc-dipeptides having different hydrophobicities, namely Fmoc-YS, Fmoc-YN, Fmoc-YL, and Fmoc-VL (the letters indicate single letter code amino acid abbreviations, for their chemical structures, see Scheme 1) were studied in 100 mM sodium phosphate buffer at pH 8.0 in the presence of various concentrations of globular proteins, β-LG and BSA. The Fmoc-dipeptides spontaneously form self-assembled structures in aqueous buffer solutions (as extensively described previously, e.g., refs 3b and 19d) and in the presence of varying concentrations of proteins. Structural characterization of the self-assembling structures was performed by circular dichroism (CD) and fluorescence spectroscopy and is shown in Figure 2.

The chiral organization of the resulting self-assembled hydrogel was studied by CD spectroscopy and the typical CD patterns of Fmoc-YL with/without different concentrations of β-LG are shown in Figure 2a with the additional spectra shown in the Supporting Information (Figures S3a, S3c, S4a, S4c, S5a, and S5c). The Fmoc- group is achiral in nature (CD silent when free in solution) but shows a strong Cotton effect when arranged in supramolecular chiral environment, detected through a characteristic peak for the fluorenyl group at 302 nm.[3b] Remarkably, it was found that the chirality of the supramolecular self-assembly changes from right-handed to left-handed with increasing protein concentration. The extent of chiral inversion is directly related to protein concentration as shown in Figure 2a. The extent and handedness of the ellipticity signal did not change upon rotating the sample holder to different angles indicating that there is no angle dependence or specific alignment of the fluorenyl groups but instead the chirality is homogenously present in supramolecular structures. Protein molecules do not show any ellipticity signal in the region of 302 nm wavelength (as shown in Figure S6a) so any signal in this area can therefore be fully assigned to supramolecular chirality of Fmoc- groups. This clearly suggests that the observed chiral inversion is solely related to peptide supramolecular chiral environment and not due to protein clusters.

The CD spectroscopy revealed that the presence of (less hydrophobic) BSA mesoscale cluster structures can also induce protein concentration dependent chiral inversion of Fmoc-YL (Figure 3a). In this case, the induced chiral order of resultant supramolecular structure was less pronounced compared to that of β-LG, suggesting a possible role for hydrophobic interactions (more on this follows later). Clearly, mesoscale protein clusters have pronounced effects on chiral organization of Fmoc-YL.

In order to study the effects of terminal amino acids, the leucine (L) was replaced with asparagine (N) and serine (S) (Scheme 1a, Fmoc-YN and Fmoc-YS). These peptide amphiphiles are expected to reduce hydrophobic interactions and provide opportunities for hydrogen bonding through the side chain (with S having one and N having two additional H-bonding sites). The nature of the side chain functionality may be expected to influence peptide−peptide interactions as well as peptide−protein interactions. The observed supramolecular chirality of Fmoc-YN structures is left-handed in the absence of β-LG (Figure 2b and S3a) and BSA (in (Figure 3b and S3c). In the presence of increasing concentrations of β-LG, the chirality also inverts but in the opposite direction compared to Fmoc-YL and the change is less pronounced. BSA directs the handedness of this system in similar fashion to β-LG but reduces, and does not invert, the chirality.

Fmoc-YS shows right handed supramolecular chirality in absence of β-LG and BSA showing reduced ellipticity in the region of 290−270 nm compared to Fmoc-YL. The addition of increasing concentrations of β-LG and BSA results in a gradual decrease of the positive (right handed) ellipticity but not the total inversion of chirality as shown in Figures 2b, 3b, S4a, and S4c. These results suggest that the extent of chiroptical control through the presence of protein clusters is reduced for less hydrophobic Fmoc-peptides. Fmoc-VL, the most hydrophobic Fmoc-peptide studied, showed the strongest supramolecular chirality and the addition of β-LG and BSA shows the strongest reduction in ellipticity, although an inversion of chirality is not observed, as depicted in Figures 2b, 3b, S5a, and S5c.

These results clearly suggest that the cooperativity between aromatic peptide amphiphiles and proteins having different hydrophobicity and hydrogen bonding tendency are important for chiral structuring leading to significant modulation of supramolecular chirality. Although there does not appear to be a simple systematic trend in these results chiral modulation of these systems is likely to be a result of the interplay of subtle differences in hydrophobicity and hydrogen bonding between peptides and proteins. In any case, there is the remarkable observation that the presence of proteins always appears to favor the opposite chirality, resulting in modulation and in some cases inversion of the chiral structure. Hence, we moved on to assess further aspects of supramolecular ordering within Fmoc-peptides, $\pi-\pi$ interactions, and subsequently investigate binding interactions between Fmoc-peptides and proteins.

Cooperative Assembly: Fmoc-Stacking. The fluorescence emission spectra for Fmoc-YL with and without β-LG and BSA showed the characteristic peaks from fluorenyl moieties at 325 nm (monomeric) and a broad peak around 420−440 nm (excimer peak)[3b] as shown in Figure 2c and 3c. The other Fmoc-peptides studied showed similar spectra but with different intensities in the order Fmoc-YN > YL > VL > YS. The monomeric emission for Fmoc-YL shows progressive quenching with increasing protein concentrations suggesting that the presence of proteins promote extended $\pi-\pi$ interactions between the fluorenyl moieties which lead to more ordered supramolecular structuring as shown previously by Ulijn et al.[3b] The other three dipeptide gelators (Fmoc-YN, -YS, -VL) showed similar trends in the presence of β-LG and BSA as shown in Figure 2d and 3d and in S3b, S3d, S4b, S4d, S5b, and S5d). The enhanced supramolecular ordering of Fmoc-dipeptides with a more hydrophobic protein β-LG (at 0.2 wt % concentration) follows the trend YL > VL > YN > YS. This indicates that more hydrophobic peptides show a more important role for π stacking interactions in self-assembly in the presence of β-LG compared to the more hydrophilic ones. A more hydrophilic protein BSA shows the trend of ordering as YN > VL > YL > YS, where the most hydrophilic peptide shows the strongest quenching in the presence of BSA. This suggests a role of protein binding with Fmoc-groups in addition to excluded volume and confinement effects of protein clusters.

Cooperative Assembly: Role of Binding Interactions. A control experiment was conducted at a Fmoc-YL concentration below that required for self-assembly/gelation (1 mM Fmoc YL in 100 mM phosphate buffer pH 8.0 with and without added β-LG at different concentrations), Figure S6.

dx.doi.org/10.1021/bm401319c | Biomacromolecules 2013, 14, 4368−4376

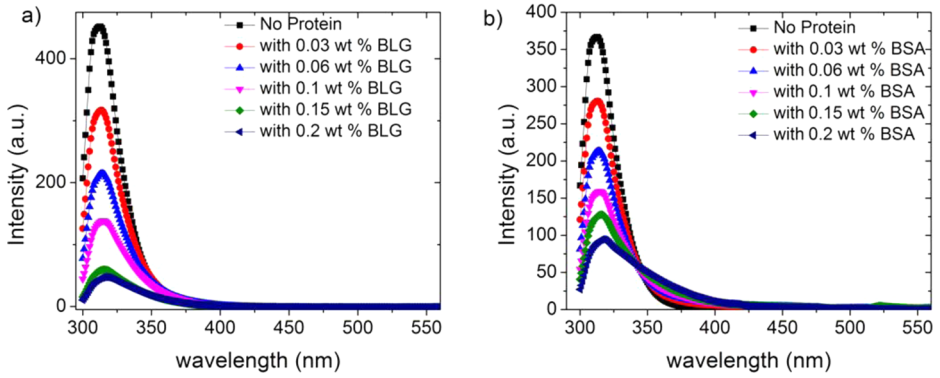

Figure 4. Fluorescence spectra of Fmoc-YL (0.06 mM) in the presence of various concentrations of BSA and β-LG in 100 mM phosphate buffer at pH 8 at room temperature to calculate the binding constants.

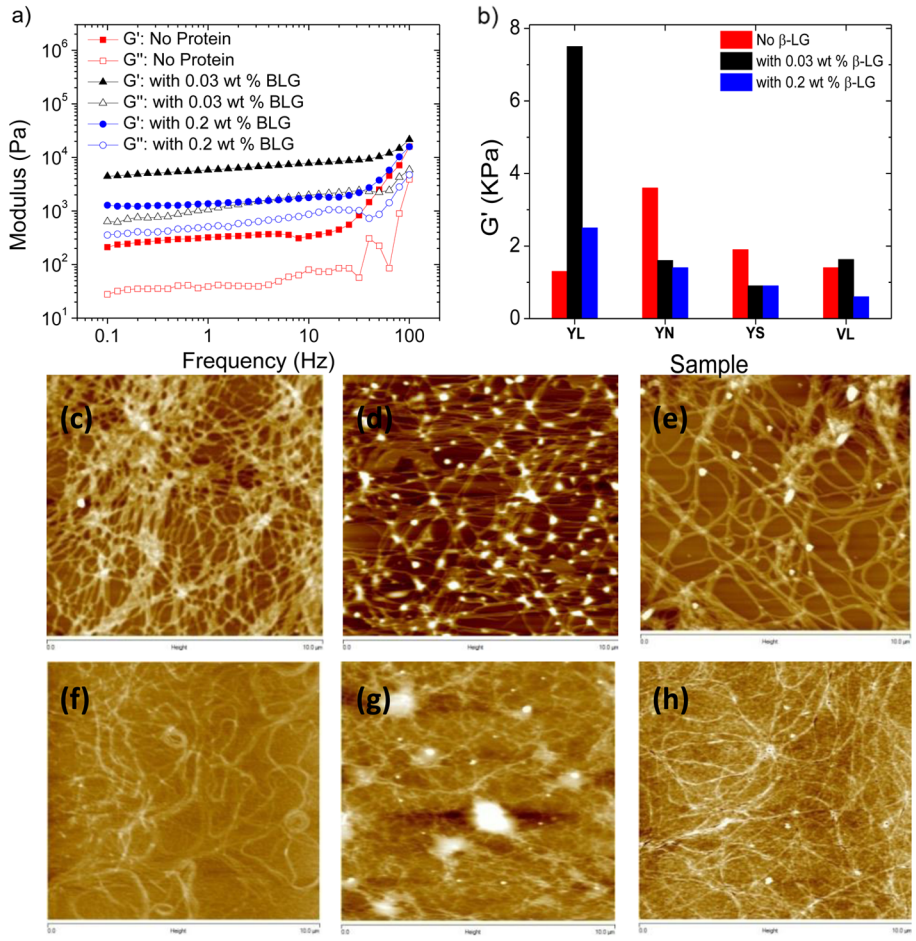

Figure 5. (a) Rheological characterization of fibrous hydrogels formed in the presence of various concentrations of β-LG: Typical frequency sweep patterns of Fmoc-YL hydrogels showing storage and loss modulus, G' and G''. (b) Storage modulus G' for hydrogels measured 24 h after of gelation for various Fmoc-dipeptides. Atomic force microscopy images of hydrogels (for YL, YN, and YS) without protein (c–e) and with 0.2 wt % β-LG (f–h): scale bar, 2 μm. The storage moduli G' for all hydrogels with different amino acid sequences and different concentrations of proteins were determined by frequency sweeps and are summarized in Table 2

The circular dichroism spectra (Figure S6a) for Fmoc-YL at various protein concentrations clearly indicate the absence of any CD signal in the region of 302 nm. We note that the peaks in region below 240 nm arise from the secondary structure of β-LG. These results confirm that the chirality observed in coassembly of peptide gelators and proteins in self-assembly conditions arise from the chiral arrangement of the Fmoc-groups arranged in fibrillar structures, with the proteins gradually reducing (and in some cases inverting) this supramolecular chirality. The fluorescence spectra for the same system (Figure S6b) show that the emission intensity of monomeric peak from Fmoc-group around 325 nm quenches after addition of β-LG suggesting the proteins in cluster structures have binding tendency with the gelator even under nonassembling conditions. These competitive interactions between the peptide gelator and protein clusters can interfere

dx.doi.org/10.1021/bm401319c | *Biomacromolecules* 2013, 14, 4368–4376

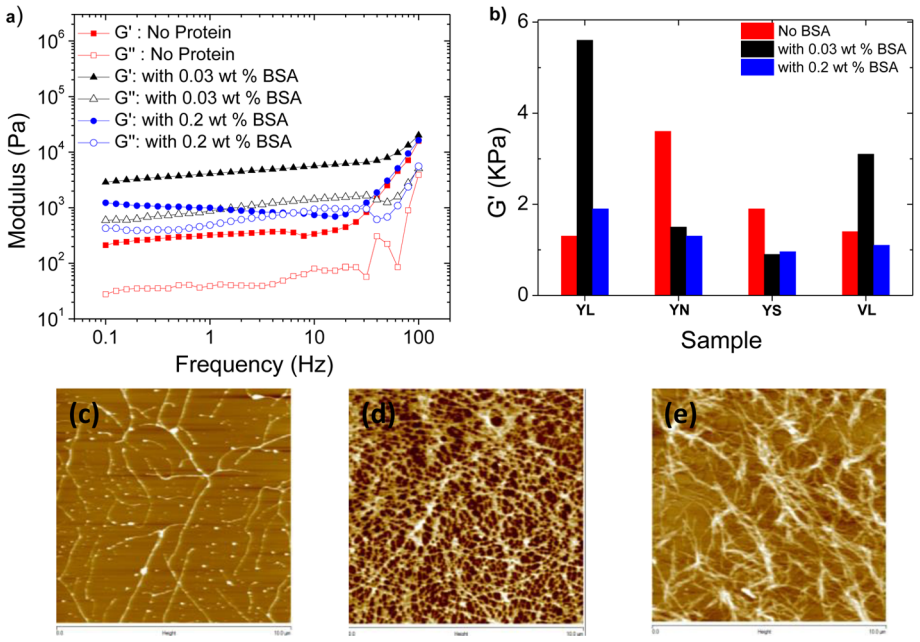

Figure 6. (a) Rheometric characterization: Typical frequency sweep patterns of Fmoc-YL hydrogels with added BSA showing storage modulus, G' and loss modulus, G''. (b) The modulation of storage modulus G' of the hydrogels with added different concentrations of BSA. Atomic force microscopy images of hydrogels with added 0.2 wt % BSA for YL (c), YN (d), and YS (e): scale bar, 2 μm.

Table 2. Storage Moduli (G') for Hydrogels Prepared with/without Addition of Various Concentrations of β-LG and BSA in 100 mM Phosphate Buffer at pH 8.0 at Room Temperature

sample	G' (kPa) with β-LG (wt %)			G' (kPa) with BSA (wt %)		
	0	0.03	0.2	0	0.03	0.2
YL	1.3 ± 0.2	7.5 ± 0.6	2.5 ± 0.3	1.3 ± 0.2	5.6 ± 0.4	1.9 ± 0.2
YN	3.6 ± 0.5	1.6 ± 0.3	1.4 ± 0.1	3.6 ± 0.4	1.5 ± 0.1	1.3 ± 0.1
YS	1.9 ± 0.1	0.9 ± 0.2	0.9 ± 0.1	1.9 ± 0.1	0.9 ± 0.1	0.9 ± 0.1
VL	1.4 ± 0.2	1.6 ± 0.2	0.6 ± 0.1	1.4 ± 0.2	3.1 ± 0.3	1.1 ± 0.2

with the nucleation process of peptide nanofibers. It is however expected that in self-assembled gel state, the interactions between Fmoc-peptides would be stronger compared to Fmoc-peptide/protein interactions, due to contributions of both $\pi-\pi$ interactions and hydrogen bonding in formation of nanofibers. Therefore, the observed cooperative self-assembly between protein and gelator molecules can also be influenced by binding of proteins with free Fmoc-peptides as well as Fmoc-peptide self-assembled structures.

The intermolecular interactions between peptides and proteins were evaluated to further elucidate the molecular mechanism of cooperative self-assembly of peptides and proteins. In order to estimate the binding interactions of Fmoc-group in the dipeptides with protein clusters, the fluorescence based method as described by Bourassa et al.[20] was applied (under low Fmoc-YL concentration of 0.06 mM, far below that required for peptide self-assembly). This method was used at a fixed concentration of Fmoc-peptide with varying protein concentrations and binding constants were calculated based on fluorescence quenching. Using this approach, both proteins show similar binding tendency to Fmoc-YL as shown in Figure 4 (Binding constants, 5.8×10^4 M^{-1} and 6×10^4 M^{-1} for β-LG and BSA, respectively). This binding is likely to play an important role in the observed cooperative self-assembly, in addition to the geometric and mobility constraints imposed by the protein clusters. Recently, Xu et al. have shown that amphiphilic peptides interact and bind with cytosol proteins in a drastically different manner depending upon their nanoscale structure.[16b]

Modulating Mechanical Properties. Having confirmed that self-assembly between Fmoc-peptides and proteins is highly cooperative, we then moved on to investigate whether these effects can be exploited to tune the structural and mechanical behavior of resulting coassembled hydrogels.

In order to study the modulation/tuning of mechanical behavior of self-assembled fibrous hydrogels with/without addition of different concentrations of proteins β-Lg and BSA, oscillatory rheology was conducted, (Figure 5 (a,b) and Figure 6a,b). Rheological measurements showed that for all hydrogels formed, the storage moduli G' exceeded the loss moduli G'', indicating that all these materials are predominantly elastic in nature. In each case, both the moduli (G' and G'') exhibit weak frequency dependence consistent with entangled polymeric network structures.[21] Both the moduli showed upturns at higher frequencies for all the hydrogels which is most likely due to the gel instability resulting from gel thickening by displacing the water from gels.[22] The characteristic frequency sweeps for the Fmoc-YL hydrogels in the presence of various concentrations of β-LG and BSA are shown in Figure 5a and 6a.

Fmoc-YL and Fmoc-VL hydrogels formed in the absence of proteins have storage moduli (G') ~ 1.3 and 1.4 kPa, respectively, which increase to 7.5 and 1.6 kPa, respectively, in the presence of 0.03 wt % β-LG concentration and the gel

dx.doi.org/10.1021/bm401319c | Biomacromolecules 2013, 14, 4368−4376

strength gradually decreases at higher protein concentrations. Similar trends were observed for both hydrogels in the presence of BSA as shown in Table 2. Fmoc-YN and Fmoc-YS (with more hydrophilic terminal amino acids) hydrogels showed different behavior in terms of gel strength modulation by both proteins. The gel strength decreased uniformly when gels were formed in the presence of increasing concentration of proteins, e.g., Fmoc-YN hydrogel had a storage modulus G' value of 3.6 kPa which decreased to 1.6 and 1.4 kPa for 0.03 and 0.2 wt % added β-LG, respectively. Similar trends were observed for both hydrogels in the presence of BSA as shown in Table 2.

These results show that self-assembled peptide fibers interact differently with protein clusters depending upon peptide residue hydrophobicity and overall protein concentration. We propose that at lower protein concentrations, the protein clusters provide primarily geometric and mobility restraint resulting in stronger Fmoc-YL and Fmoc-VL hydrogels. At higher protein concentrations the peptide−protein interactions become more significant resulting in the appearance of thicker fibers for hydrophobic protein β-LG (not with BSA), which may be due to protein coating (Figure 6, parts c and f, and Table3) resulting in softening of the resulting gels.

Table 3. Summary of Widths of the Fmoc-YL, Fmoc-YN, and Fmoc-YS Hydrogels Fibers Prepared with/without Addition of 0.2 wt % of β-LG or BSA in 100 mM Phosphate Buffer at pH 8.0 at RT

sample	fiber width (nm) without/with β-LG (wt %)		fiber width (nm) with BSA (wt %)
	0	0.2	0.2
YL	70−130	60−160	60−100
YN	60−120	120−240	140−270
YS	150−240	70−95	120−270

The decrease in gel strength of Fmoc-YN and Fmoc-YS formed in the presence of increasing concentration of proteins may be due to the stronger interactions with proteins. In general, more hydrophilic peptides resulted in enhanced fiber thickness with increased protein concentration (Figure 5c−h, Figure 6c−e, and Table 3), suggesting that the nature and the concentration of the protein has impact on the fiber morphology. It has been shown by Murphy et al. that the protein conformations play important role in the gel properties and functional materials can be designed based on the selection of protein conformations.[23]

CONCLUSIONS

The self-assembly process of Fmoc-dipeptides is influenced by co-operative effects of geometrical/mobility restrictions of peptide gelators in presence of protein fractal cluster structures and also due to the intermolecular interactions (leading to structural differences in nucleation process of fiber growth formation) resulting in different structural and mechanical properties of the self-assembled hydrogels.

Recently, Meijer et al. have shown that self-assembly of left-handed helical stacks of π-conjugated oligomers formed through a thermodynamically controlled pathway competed with formation of right-handed aggregates formed through a kinetically control pathway and this process could be directed toward kinetic control by an addition of chiral auxiliary molecule.[24]

To our knowledge it is first time reported here that the mesoscale protein clusters achieved at very low protein concentrations at room temperature and at pH near physiological conditions can modulate the peptide self-assembly process. While the detailed mechanism still needs to be explored by employing time-dependent *in situ* spectroscopic and scattering characterization techniques, it is clear that protein/peptide coassembly provides a new direction to control/modulate the molecular level of chiral organization and supramolecular ordering resulting in different viscoelastic behavior of hydrogels. We believe that these principles are quite general and can be employed to a wide range of self-assembling systems to control or fine-tune the structural and mechanical properties of the nanostructured materials for biomedical applications where proteins and peptides coexist.[25] In addition, fundamental insights into cooperative interplay of molecular interactions and confinement by clusters of chiral macromolecules is relevant to gaining understanding of the molecular mechanisms of relevance to the origin of life and development of synthetic mimics of living systems.[26]

ASSOCIATED CONTENT

Supporting Information

Data for dynamic light scattering measurements for different concentrations of BSA and β-LG in 10 mM and 100 mM phosphate buffer (Figures S1 and S2), spectroscopic characterizations of self-assembly processes of Fmoc-YN, Fmoc-YS, and Fmoc-VL in the presence of various concentrations of proteins (Figures S3−S5), and spectroscopic characterization of Fmoc-YL in nonself-assembling conditions (1 mM) in the presence of various concentrations of β-LG (Figure S6). This material is available free of charge via the Internet at http://pubs.acs.org.

AUTHOR INFORMATION

Corresponding Authors

*E-mail: (J.S.) jan.sefcik@strath.ac.uk.

*E-mail: (R.V.U.) rein.ulijn@strath.ac.uk.

Author Contributions

N.J. performed the experiments and analyzed the data. The manuscript was written through contributions of all authors. All authors have given approval to the final version of the manuscript.

Notes

The authors declare no competing financial interest.

ACKNOWLEDGMENTS

This work was supported by a BBSRC research grant, Number BB/J021113/1. The research leading to these results has received funding from the European Research Council under the European Union's Seventh Framework Programme (FP7/2007−2013)/ERC Grant Agreement No. 258775 (EMERgE).

REFERENCES

(1) (a) Lehn, J. M.; *Supramolecular Chemistry − concepts and perspectives*: VCH: Weinheim, Germany, 1995; (b) Whitesides, G. M.; Grzybowski, B. *Science* **2002**, *295*, 2418−21. (c) Aida, T.; Meijer, E. W.; Stupp, S. I. *Science* **2012**, *335*, 813−817. (d) Fichman, G.; Gazit, E. *Acta Biomater.* **2013**, DOI: DOI: 10.1016/j.bbr.2011.03.031.

(2) (a) Zhang, S. *Nat. Biotechnol.* **2003**, *21*, 1171−78. (b) Boyle, A. L.; Woolfson, D. N. *Chem. Soc. Rev.* **2011**, *40*, 4295−4306.

(3) (a) Yang, Z.; Gu, H.; Fu, D.; Gao, P.; Lam, J. K.; Xu, B. *Adv. Mater.* **2004**, *16*, 1440−1444. (b) Hirst, A. R.; Roy, S.; Arora, M.; Das, A. K.; Hodson, N.; Murray, P.; Marshall, S.; Javid, N.; Sefcik, J.;

Boekhoven, J.; van Esch, J. H.; Santabarbara, S.; Hunt, N. T.; Ulijn, R. V. *Nat. Chem.* **2010**, *2*, 1089−1094. (c) Gao, Y.; Shi, J.; Yuan, D.; Xu, B. *Nat. Commun.* **2012**, *3*, 1033. (d) Hirst, A. R.; Escuder, B.; Miravet, J. F.; Smith, D. K. *Angew. Chem., Int. Ed.* **2008**, *47*, 8002−8020. (e) Fleming, S.; Debnath, S.; Frederix, P. W. J. M.; Tuttle, T.; Ulijn, R. V. *Chem. Commun.* **2013**, *49*, 10587−10589.
(4) Ellis, R. J.; Minton, A. P. *Nature* **2003**, *425*, 27−28.
(5) Minton, A. P. *Curr. Opi. in Str. Biol.* **2000**, *10*, 34−39.
(6) (a) Ellis, R. J. *Trends Biochem. Sci.* **2001**, *26*, 597−604. (b) Zimmerman, S. B.; Minton, A. P. *Annu. Rev. Biophys. Biomol. Struct.* **1993**, *22*, 27−65.
(7) Stradner, A.; Sedgwick, H.; Cardinaux, F.; Poon, W. C. K.; Egelhaff, S. U.; Schurtenberger, P. *Nature* **2004**, *432*, 492−95.
(8) Javid, N.; Vogtt, K.; Roy, S.; Hirst, A. R.; Hoell, A.; Hamley, I. W.; Ulijn, R. V.; Sefcik, J. *J. Phys. Chem. Lett.* **2011**, *2*, 1395−99.
(9) Hagiwara, T.; Kumagari, H.; Nakamura, K. *Biosci. Biotech. Biochem.* **1996**, *60* (11), 1757−63.
(10) Krebs, M. R. H.; Bromley, E. H. C.; Rogers, S. S.; Donald, A. M. *Biophys. J.* **2005**, *88*, 2013−2021.
(11) Grudzielanek, S.; Velkova, A.; Shukla, A.; Smirnovas, V.; Tatarek-Nossol, M.; Rehage, H.; Kapurniotu, A.; Winter, R. *J. Mol. Biol.* **2007**, *370*, 372−384.
(12) Yan, H.; Frielinghaus, H.; Nykanen, A.; Ruokolainen, J.; Saiani, A.; Miller, A. F. *Soft Matter* **2008**, *4*, 1313−1325.
(13) Pan, W.; Filobelo, L.; Pham, N. D.; Galkin, O.; Uzunova, V. V.; Vekilov, P. G. *Phys. Rev. Lett.* **2009**, *102*, 058101−4.
(14) (a) Rozkiewicz, D. I.; Myers, B. D.; Stupp, S. I. *Angew. Chem., Int. Ed.* **2011**, *50*, 6324−6327. (b) Capito, R. M.; Azevedo, H. S.; Velichko, Y. S.; Mata, A.; Stupp, S. I. *Science* **2008**, *139*, 1812−16.
(15) (a) Chen, L.; Revel, S.; Morris, K.; Spiller, D. G.; Serpell, L. C.; Adams, D. J. *Chem. Commun.* **2010**, *46*, 6738−40. (b) Wang, Q.; Mynar, J. L.; Yoshida, M.; Lee, E.; Lee, M.; Okuro, K.; Kinbara, K.; Aida, T. *Nature* **2010**, *463*, 339−343.
(16) (a) Stuart, M.; van Bommel, K.; Friggeri, A.; de Jong, M.; van Esch, J. *Angew. Chem., Int. Ed.* **2008**, *47*, 2063−2066. (b) Kuang, Y.; Yuan, D.; Zhang, Y.; Kao, A.; Du, X.; Xu, B. *RSC. Adv.* **2013**, *3*, 7704−7707.
(17) Kyte, J.; Doolittle, R. F. *J. Mol. Biol.* **1982**, *157*, 105−32.
(18) (a) Sandkuhler, P.; Lattuada, M.; Wu, H.; Sefcik, J.; Morbidelli, M. *Adv. Colloid Interface Sci.* **2005**, *113*, 65−83. (b) Sandkuhler, P.; Sefcik, J.; Morbidelli, M. *Langmuir* **2005**, *21* (5), 2062−2077.
(19) (a) Adams, D. J.; Topham, P. D. *Soft Matter* **2010**, *6*, 3707−3721. (b) Ryan, D. M.; Nilsson, B. L. *Polymer Chem.* **2012**, *3*, 18−33. (c) Zelzer, M.; Ulijn, R. V. *Chem. Soc. Rev.* **2010**, *39*, 3351−3357. (d) Hughes, M.; Birchall, L. S.; Zuberi, K.; Aitkin, L. A.; Debnath, S.; Javid, N.; Ulijn, R. V. *Soft Matter* **2012**, *8*, 11565−11574.
(20) Bourassa, P.; Dubeau, S.; Maharvi, G. M.; Fauq, A. H.; Thomas, T. J.; Tajmir-Riahi, H. A. *Eur. J. Med. Chem.* **2011**, *46*, 4344−53.
(21) Tang, C.; R. V. Ulijn, R. V.; Saiani, A. *Langmuir* **2011**, *27*, 14438−14449.
(22) Cheng, G.; Castelletto, V.; Moulton, C. M.; Newby, G. E.; Hamley, I. W. *Langmuir* **2010**, *26*, 4990−98.
(23) Murphy, W. L.; Dillmore, W. S.; Modica, J.; Mrksich, M. *Angew. Chem., Int. Ed.* **2007**, *46*, 3066−3069.
(24) Korevaar, P. A.; George, S. J.; Markvoort, A. J.; Smulders, M. M. J.; Hilberts, P. A. J.; Schenning, A. P. H. J.; De Greef, T. F. A.; Meijer, E. W. *Nature* **2012**, *481*, 492−496.
(25) (a) Banwell, E. F.; Abelardo, E. S.; Adams, D. J.; Birchall, M. A.; Corrigan, A.; Donald, A. M.; Kirkland, M.; Serpell, L. C.; Butler, M. F.; Woolfson, D. N. *Nat. Mater.* **2009**, *8*, 596−600. (b) Silva, G. A.; Czeisler, C.; Niece, K. L.; Beniash, E.; Kessler, J. A.; Stupp, S. I. *Science* **2004**, *303*, 1352−1355.
(26) Mann, S. *Angew. Chem., Int. Ed.* **2013**, *52*, 155−162.